Research Square

Preprints are preliminary reports that have not undergone peer review.
They should not be considered conclusive, used to inform clinical practice,
or referenced by the media as validated information.

Early right ventricular enlargement is associated with subsequent lactate burden in sepsis

Yiyuanzi Zhao
Dongzhimen Hospital Affiliated to Beijing University of Chinese Medicine
Jiaqi Wang
Dongzhimen Hospital Affiliated to Beijing University of Chinese Medicine
Xue Gong
Dongzhimen Hospital Affiliated to Beijing University of Chinese Medicine
Wei Bi
Dongzhimen Hospital Affiliated to Beijing University of Chinese Medicine
Caijun Wu
2054143218@qq.com

Dongzhimen Hospital Affiliated to Beijing University of Chinese Medicine

Article

Keywords: sepsis, lactate, right ventricular enlargement, echocardiography, hemodynamics, metabolic recovery

Posted Date: November 27th, 2026

DOI: https://doi.org/10.21203/rs.3.rs-11649179/v1

License: This work is licensed under a Creative Commons Attribution 4.0 International License.
Read Full License

Additional Declarations: No competing interests reported.

Abstract

Lactate and bedside echocardiography provide complementary information in sepsis, but whether early cardiac structure is associated with subsequent metabolic recovery is uncertain. We analyzed a time-ordered Sepsis-3 cohort using MIMIC-IV v3.1 and MIMIC-IV-Echo v1.0.1. Early transthoracic echocardiography (E1) was performed within 18 h of ICU admission; Lpre was the last lactate within 6 h before E1, and L24 was the lactate closest to 24 h, with E1 at least 6 h before L24. Among 998 eligible patients, 898 had an RV chamber-size grade. Each one-grade increase in RV chamber-size severity was associated with a 5.42% higher subsequent L24 geometric mean (95% CI 0.47–10.62%; P = 0.031) after adjustment for Lpre, illness severity, comorbidities, and measurement timing. A 10-percentage-point lower LVEF showed a near-null association (+ 0.37%, 95% CI − 1.41 to 2.18%; P = 0.685), and the RV association persisted in the joint model. Estimates were directionally consistent across sensitivity analyses. Early RV enlargement was therefore associated with greater subsequent lactate burden after accounting for preceding lactate, supporting RV chamber size as a candidate cardiocirculatory phenotype for prospective validation.

Introduction

Blood lactate is a dynamic marker of systemic stress in sepsis and is influenced by tissue oxygen delivery, adrenergically driven glycolysis, mitochondrial and metabolic responses, and lactate clearance [1, 2]. Serial measurement is therefore clinically informative because persistent elevation after initial resuscitation can indicate that physiological recovery remains incomplete. Randomized and observational work has also shown that lactate trajectory does not map one-to-one onto macrocirculatory variables, underscoring the need to interpret lactate within a broader physiological context [3–6]. A clinically useful translational question is whether an early, readily available cardiac phenotype can help identify patients whose metabolic recovery remains impaired several hours later.

Sepsis-related cardiac involvement is heterogeneous and extends beyond reduced left ventricular ejection fraction (LVEF) [7, 8]. The right ventricle (RV) may be particularly informative because its size and function integrate several features of the cardiopulmonary circulation, including pulmonary vascular afterload, positive-pressure ventilation, volume and pressure loading, venous congestion, and ventricular interaction [9–11]. Contemporary phenotyping studies have further suggested that RV-predominant abnormalities define clinically meaningful subgroups in sepsis and critical illness [12, 13]. Unlike LVEF, which is strongly load dependent and may remain preserved in vasodilatory states, RV enlargement may therefore serve as a bedside marker of a broader cardiocirculatory state.

Most available studies, however, relate echocardiographic findings and lactate measured at similar time points or use mortality as the principal endpoint. Such designs cannot determine whether an early cardiac phenotype carries information about a subsequent metabolic trajectory beyond the contemporaneous lactate value. The key gap is thus temporal: whether an RV structural phenotype

identified early in the ICU course remains associated with lactate measured later after conditioning on the lactate level immediately preceding echocardiography.

We therefore constructed a strictly time-ordered Lpre→E1→L24 framework using MIMIC-IV and MIMIC-IV-Echo. Early RV chamber-size severity was the primary cardiac phenotype and subsequent L24 lactate burden was the primary outcome; LVEF, qualitative RV function, tricuspid regurgitation velocity, and E/e' were evaluated as physiological comparators. We hypothesized that greater early RV enlargement would remain associated with higher subsequent lactate burden after adjustment for pre-echocardiography lactate and prespecified clinical covariates, supporting a candidate cardiocirculatory phenotype of impaired metabolic recovery.

Methods

Study design and data sources

We conducted a retrospective cohort study using MIMIC-IV v3.1 and MIMIC-IV-Echo v1.0.1 [14, 15]. The sepsis population was defined according to the Sepsis-3 framework [16]. Only the first eligible ICU stay for each patient was retained, and the prespecified etiologic cardiac exclusion rules were maintained. MIMIC-IV and MIMIC-IV-Echo contain deidentified data available through credentialed PhysioNet access. The original MIMIC data collection was approved by the institutional review boards of the Massachusetts Institute of Technology and Beth Israel Deaconess Medical Center, with the requirement for individual informed consent waived. This secondary analysis used only deidentified data under the applicable PhysioNet data-use requirements.

Time-ordered primary analysis cohort

To ensure that the exposure preceded the primary outcome, the main analysis required: (1) an E1 transthoracic echocardiogram (TTE) performed 0–18 h after ICU admission; (2) at least one lactate measurement within the 6 h before E1, with the last measurement designated Lpre; (3) a SOFA index time no later than E1; (4) an L24 value defined as the lactate measurement closest to 24 h within 18–30 h after ICU admission; and (5) E1 preceding L24 by at least 6 h. This time-ordered cohort was embedded within the Sepsis-3 population [16]. The primary RV analysis additionally required a mappable structured RV chamber-size result at E1.

Early echocardiographic phenotypes

The primary exposure was obtained from the structured clinical echocardiography record for the selected E1 examination in MIMIC-IV-Echo [15] and was defined as RV chamber-size severity: normal/small = 0, mild or nonspecific enlargement = 1, moderate enlargement = 2, and severe enlargement = 3. This variable represents the interpreting clinician's integrated structural assessment

rather than a core-laboratory remeasurement of a single RV dimension. Comparator phenotypes were LVEF (per 10-percentage-point decrease), qualitative RV dysfunction, TR velocity (per 0.5-m/s increase, as a proxy for pulmonary vascular afterload), and mean E/e' (per 5-unit increase). Use of TR velocity as part of right-heart and pulmonary-circulation assessment is consistent with current echocardiographic guidance [9]. Mean E/e' was calculated as mitral E velocity divided by the mean of septal and lateral e', using component measures and chamber-quantification principles consistent with standard echocardiographic frameworks [17]. Because structured-field availability in MIMIC-IV-Echo varies with source system and clinical reporting, an absent or unmappable structured value was classified as phenotype unavailable. Echocardiographic phenotypes were analyzed using complete cases for the corresponding phenotype, with the model-specific sample size reported for each analysis. RV-grade mapping and phenotype availability are detailed in Supplementary Table S1.

Lactate outcomes

The primary outcome was continuous L24, modeled after natural-log transformation; regression coefficients were back-transformed and reported as percentage differences in the geometric mean. Because the primary model adjusted for log(Lpre), the effect estimate represents the association of the early cardiac phenotype with subsequent L24 burden among patients with similar pre-echocardiography lactate levels. Among patients with Lpre > 2 mmol/L, persistent hyperlactatemia was defined as L24 > 2 mmol/L. A transition from Lpre ≤ 2 to L24 > 2 mmol/L was examined only as an exploratory delayed-rise pattern.

Covariate adjustment

The primary model adjusted for age, sex, early SOFA score (SOFA6), heart failure, coronary artery disease, atrial fibrillation, diabetes, chronic kidney disease (CKD), chronic obstructive pulmonary disease (COPD), chronic liver disease, ICU service type, admission type, time from ICU admission to E1, time from Lpre to E1, and time from ICU admission to L24. SOFA6 was taken from the locked early-SOFA field, with its index time required to be no later than E1. All time-varying covariates in the primary adjustment set were restricted to information available before E1 to preserve temporal ordering.

Statistical analysis

The primary analysis used ordinary least squares regression with HC3 heteroskedasticity-consistent standard errors. Log(L24) was the outcome, RV chamber-size severity was the primary exposure, and log(Lpre) plus the prespecified covariates formed the adjustment set. RV chamber size was modeled primarily as an ordinal variable from 0 to 3; effect estimates are reported as the percentage change in L24 per one-grade increase, with 95% confidence intervals (CIs). To assess whether equal spacing of the ordinal grades oversimplified the observed pattern, RV chamber size was also modeled categorically in four levels, and covariate-adjusted marginal geometric means of L24 were reported. Because the severe

group included only 19 patients, the categorical model was used primarily to assess the overall pattern and display marginal means rather than to support grade-specific pairwise conclusions. Comparator phenotypes were analyzed within the same covariate framework, and Benjamini–Hochberg false-discovery rate (BH-FDR) adjustment was used as a secondary aid to interpret multiple comparator analyses. A joint RV chamber-size/LVEF model was also fitted to assess whether the RV association persisted after accounting for contemporaneous LV systolic-function information.

Persistent hyperlactatemia was analyzed using modified Poisson regression with robust standard errors and reported as a prevalence ratio (PR). Prespecified sensitivity analyses included E1 ≤ 12 h, an E1-to-L24 interval ≥ 9 h, binary RV enlargement, the alternative outcome log(L24/Lpre), exclusions related to pulmonary hypertension or pulmonary embolism, a stricter cardiogenic-shock exclusion, and additional adjustment for pre-E1 invasive ventilation, vasoactive therapy, mean arterial pressure (MAP), positive end-expiratory pressure (PEEP), and recorded net fluid balance. To address renal function and treatment-related confounding, additional analyses incorporated pre-E1 renal SOFA, epinephrine exposure, and active renal replacement therapy (RRT), with restriction analyses excluding severe renal SOFA or pre-existing CKD. Epinephrine exposure, active RRT, and recorded net fluid balance occurring between E1 and L24 were evaluated separately as exploratory analyses of post-exposure treatment pathways and were kept distinct from the pre-E1 baseline confounder adjustment. Sensitivity analyses were interpreted primarily according to the consistency of effect direction, magnitude, and confidence intervals.

Secondary model-form and distributional analyses

After the primary model had been locked, two secondary analyses were used to assess whether the observed RV association was dependent on conventional linear model specification. Quantile regression examined the association across the 25th, 50th, 75th, and 90th conditional percentiles of L24 [18]. Cross-fitted double/debiased machine learning (DML) estimated an orthogonalized partial linear association using out-of-fold nuisance-function prediction [19]. These analyses retained the same exposure, outcome, temporal definition, and covariate set as the primary analysis and were interpreted as model-form and distributional checks rather than independent confirmatory endpoints.

Downstream clinical relevance

In-hospital mortality was examined only in secondary analyses intended to assess the clinical relevance of subsequent lactate burden. First, modified Poisson regression compared the risk of in-hospital death for L24 > 2 versus ≤ 2 mmol/L, adjusting for Lpre, age, sex, early SOFA, major comorbidities, ICU service type, admission type, and prespecified measurement-timing variables. Second, the L24 measurement time was used as a landmark, and Cox regression evaluated the association of continuous L24 burden with subsequent in-hospital mortality. A cumulative-incidence analysis treating live hospital discharge as a competing event was used as a sensitivity analysis [20]. These analyses were intended to evaluate the

downstream clinical relevance of L24 rather than causal mediation; the modified Poisson, landmark Cox, and competing-risk results are reported in Supplementary Tables S7, S6, and S11, respectively.

Reporting standards

The study was reported in accordance with the STROBE statement for observational studies [21] and the RECORD extension for routinely collected health data [22]. For the newly specified time-ordered primary analysis, the time windows, primary outcome, and primary adjustment framework were locked before formal rerunning. However, selection of RV chamber size as the primary cardiac phenotype was informed by earlier exploratory work in the same database; the present study should therefore be considered discovery-oriented and requires independent external validation.

Use of artificial intelligence tools

No artificial intelligence (AI) tools were used in the preparation, writing, editing, or analysis of this manuscript.

Results

Time-ordered cohort

The original Sepsis-3 early-echocardiography source cohort included 2,663 patients. After applying the E1 0–18-h window, requiring SOFA time ≤E1, and requiring an E1-to-L24 interval of at least 6 h, 1,234 patients remained. Of these, 998 had an available Lpre measurement within 6 h before E1, and 898 had a mappable RV chamber-size grade and entered the primary analysis (Fig. 1).

Baseline characteristics

Baseline characteristics of the time-ordered primary cohort, stratified by the presence of RV enlargement, are summarized in Table 1.

Table 1
Baseline characteristics of the time-ordered primary cohort, stratified by RV enlargement.

Variable	Overall	No RV enlargement	RV enlargement	SMD
Age, y	67.0 [55.0, 77.8]	65.0 [52.0, 76.0]	69.0 [60.0, 79.0]	0.2857
SOFA	4.0 [3.0, 6.0]	4.0 [3.0, 6.0]	4.0 [3.0, 6.0]	0.02517
Pre-E1 lactate, mmol/L	2.7 [1.7, 4.6]	2.6 [1.7, 4.5]	2.7 [1.6, 4.7]	0.02577
Subsequent L24 lactate, mmol/L	1.9 [1.3, 3.4]	1.8 [1.3, 3.3]	2.0 [1.4, 3.5]	0.04136
E1 timing from ICU admission, h	9.5 [6.1, 13.2]	10.0 [6.2, 13.4]	9.2 [5.5, 12.8]	-0.134
E1→L24 interval, h	14.2 [10.6, 17.9]	13.9 [10.5, 17.6]	14.8 [10.7, 18.1]	0.1109
Male	521 (58.0%)	319 (55.9%)	202 (61.8%)	0.12
Heart failure	433 (48.2%)	232 (40.6%)	201 (61.5%)	0.4168
Coronary artery disease	299 (33.3%)	185 (32.4%)	114 (34.9%)	0.05213
Atrial fibrillation	386 (43.0%)	206 (36.1%)	180 (55.0%)	0.3809
Diabetes	358 (39.9%)	227 (39.8%)	131 (40.1%)	0.006256
Chronic kidney disease	318 (35.4%)	175 (30.6%)	143 (43.7%)	0.2707
COPD	170 (18.9%)	92 (16.1%)	78 (23.9%)	0.1936
Chronic liver disease	141 (15.7%)	85 (14.9%)	56 (17.1%)	0.06107
Pre-E1 invasive ventilation	610 (67.9%)	388 (68.0%)	222 (67.9%)	-0.001308
Pre-E1 vasoactive exposure	645 (71.8%)	401 (70.2%)	244 (74.6%)	0.09823

Primary association between RV structural grade and subsequent L24

In the primary model, each one-grade increase in RV chamber-size severity was associated with a 5.42% higher subsequent L24 geometric mean (95% CI 0.47%–10.62%; P = 0.031; Fig. 3; Supplementary Table S2). By comparison, each 10-percentage-point lower LVEF corresponded to a 0.37% higher L24 (95% CI −1.41% to 2.18%; P = 0.685), and the estimates for qualitative RV dysfunction and TR velocity were likewise close to null. Mean E/e' showed a nominal inverse association, but the evidence weakened after FDR adjustment. When RV chamber size and LVEF were entered simultaneously, the RV association persisted (+ 5.42%; P = 0.032), whereas the LVEF association remained near null (P = 0.960;

Supplementary Table S3), indicating that the RV structural signal carried statistical information beyond contemporaneous LVEF.

Patient-level data are shown in Fig. 2. In the categorical check of the ordinal RV coding, marginal standardization yielded adjusted L24 geometric means of approximately 2.15, 2.23, 2.49, and 2.44 mmol/L for normal, mild, moderate, and severe RV grades, respectively (Supplementary Table S4). The overall pattern was directionally consistent with the primary ordinal estimate. However, the severe group contained only 19 patients, had a wide confidence interval, and showed a mean close to that of grade 2; accordingly, the categorical results were interpreted as supporting an overall graded/ordinal pattern rather than a strictly monotonic stepwise dose-response.

Secondary model-form and distributional analyses

The secondary model-form analyses were concordant with the primary result. DML estimated a 6.28% higher subsequent L24 per one-grade increase in RV chamber size (95% CI 1.34%–11.45%; P = 0.012), and the RV estimate remained similar in the joint RV/LVEF DML model (Supplementary Table S9).

Quantile regression suggested heterogeneity across the conditional L24 distribution. Associations were smaller at the 25th and 50th percentiles and larger in the upper tail (75th percentile: +5.50%, P = 0.042; 90th percentile: +9.83%, P = 0.014; Supplementary Table S10). These analyses were secondary and are presented as support for the robustness and distributional interpretation of the primary association. These secondary model-form and distributional findings are summarized in Fig. 4.

Persistent hyperlactatemia and downstream clinical relevance

Among 572 patients with Lpre > 2 mmol/L and available RV chamber-size data, 368 remained above 2 mmol/L at L24. Each one-grade increase in RV chamber size was associated with a directionally concordant but borderline higher prevalence of persistent hyperlactatemia (PR = 1.069, 95% CI 0.996–1.149; P = 0.066; Supplementary Table S5).

Among 896 patients with RV structural data and aligned timing records, 351 died in hospital. Crude in-hospital mortality was 28.0% among patients with L24 ≤ 2 mmol/L and 52.6% among those with L24 > 2 mmol/L. After adjustment for Lpre, age, sex, early SOFA, major comorbidities, ICU service type, admission type, and measurement timing, L24 > 2 mmol/L remained associated with higher in-hospital mortality (adjusted PR = 1.39, 95% CI 1.14–1.71; P = 0.001; Supplementary Table S7).

In the L24-landmark Cox analysis, each doubling of L24 was associated with a higher hazard of subsequent in-hospital death (HR = 1.68, 95% CI 1.43–1.98; P < 0.001), whereas the direct association of RV chamber size with mortality was weaker (HR = 1.16, 95% CI 0.99–1.34; P = 0.059; Supplementary Table S6). The gradient associated with L24 persisted when live hospital discharge was treated as a

competing event (Supplementary Table S11), supporting subsequent lactate burden as a clinically meaningful metabolic outcome.

Sensitivity analyses

Point estimates remained positive across sensitivity analyses. Restricting E1 to ≤ 12 h or requiring an E1-to-L24 interval ≥ 9 h, excluding a history of pulmonary hypertension or current pulmonary embolism, applying a stricter cardiogenic-shock exclusion, and further adjusting for pre-E1 invasive ventilation, vasoactive therapy, PEEP, MAP, or recorded net fluid balance all yielded estimates directionally consistent with the primary analysis. In renal-function sensitivity analyses, explicit adjustment for the pre-E1 renal SOFA component yielded an RV estimate of + 5.32% (95% CI 0.36%–10.52%; P = 0.036). Excluding severe renal SOFA ≥ 3 or pre-existing CKD yielded estimates of + 5.16% and + 4.62%, respectively, with the direction preserved. Additional adjustment for pre-E1 epinephrine exposure, active RRT, or both produced RV estimates of + 5.38% (95% CI 0.44%–10.57%), + 5.25% (95% CI 0.31%–10.44%), and + 5.31% (95% CI 0.38%–10.49%), respectively, closely matching the locked primary estimate (Supplementary Table S8; Supplementary Fig. S1).

In exploratory post-exposure analyses, adding epinephrine exposure, active RRT, or recorded net fluid balance measured between E1 and L24 yielded RV estimates of + 5.69%, + 4.49%, and + 4.78%, respectively; the combined treatment-pathway model yielded + 4.50% (95% CI − 0.25% to 9.48%; P = 0.064). Although the estimates were modestly attenuated, they remained positive. Because these variables were measured after E1, these results are presented separately as exploratory treatment-pathway analyses describing the stability of the RV estimate under evolving treatment conditions (Supplementary Table S12).

Discussion

The principal finding is that an early RV structural phenotype was associated with subsequent lactate burden after conditioning on the lactate level immediately before echocardiography and on prespecified markers of illness severity and clinical context. The corresponding LVEF association was near null, and the RV signal persisted when both measures were entered together. This pattern suggests that early RV chamber size may capture a cardiocirculatory dimension of sepsis that is not represented by LVEF alone and that remains relevant to metabolic recovery several hours later. The result is best viewed as phenotype-level evidence rather than as proof of a direct causal effect of RV enlargement on lactate.

The translational contribution of this study lies primarily in the temporal design. Cross-sectional coexistence of RV abnormality and hyperlactatemia is difficult to interpret because both can reflect the same moment of severe illness. By ordering the measurements as Lpre, E1, and L24, requiring E1 to precede L24 by at least 6 h, and adjusting for Lpre, we asked whether the echocardiographic phenotype added information about a later lactate state beyond the immediately preceding lactate concentration. This design does not establish causality, but it narrows the interpretation from simple contemporaneous correlation toward a sequential clinical phenotype–trajectory relationship.

The RV is highly sensitive to pulmonary vascular afterload, pressure and volume loading, and positive-pressure ventilation [9]. In septic shock, RV dilatation may coexist with venous congestion and impaired forward flow even when conventional LV systolic function appears preserved [10, 23]. These features provide a plausible physiological basis for an RV structural signal to track later lactate burden: the RV may integrate pulmonary vascular stress, ventricular interaction, preload distribution, and systemic venous congestion, all of which can influence effective organ perfusion and lactate clearance. The near-null LVEF comparator is consistent with the known load dependence of LVEF in vasodilatory critical illness and supports multidimensional rather than LVEF-centered cardiac phenotyping [7, 24, 25].

The secondary DML estimate was close to the primary estimate, reducing concern that the finding was driven entirely by the functional form chosen for conventional covariate adjustment. Quantile regression suggested that the association may be more apparent in the upper portion of the subsequent lactate distribution. This pattern is compatible with the idea that RV enlargement marks a phenotype most relevant among patients with more pronounced persistent metabolic stress, but these distributional analyses were exploratory and require replication.

RV chamber size is not a mechanism-specific marker. It may integrate ARDS, PEEP exposure, intravascular volume, pulmonary vascular disease, renal dysfunction, and overall circulatory severity. We therefore examined several of these alternative explanations through prespecified exclusions and sensitivity analyses involving mechanical ventilation, vasoactive therapy, MAP, PEEP, recorded fluid balance, renal SOFA, epinephrine, and active RRT. The direction and magnitude of the RV estimate were generally stable, while exploratory E1-to-L24 treatment-pathway analyses produced modest attenuation without reversal. Residual and unmeasured confounding nonetheless remains possible, particularly for venous congestion, pulmonary vascular resistance, RV–pulmonary artery coupling, detailed fluid exposure, and treatment intensity.

The subsequent lactate state was clinically consequential: in-hospital mortality exceeded 50% among patients with L24 > 2 mmol/L, and the adjusted association between elevated L24 and mortality remained strong. The landmark analysis yielded a concordant relationship between continuous L24 and subsequent death. In contrast, the direct RV–mortality association was weaker. This separation is informative because the study was designed to identify a cardiocirculatory phenotype linked to later metabolic stress rather than to establish RV enlargement as an independent mortality predictor.

Prior work has established that RV dysfunction and enlargement occur in sepsis and can be associated with adverse outcomes [10, 11, 26]. More recent latent-profile analyses have emphasized the heterogeneity of septic cardiac phenotypes, including RV-predominant patterns [12]. Lactate studies have similarly moved from single measurements toward trajectories and joint physiological patterns [28, 29]. Our findings connect these two lines of investigation by placing a routinely available RV structural phenotype before a subsequent lactate measurement while conditioning on the pre-echocardiography lactate level. This phenotype–trajectory framing is complementary to mortality-centered studies and may be useful for future prospective multimodal phenotyping.

The findings do not establish RV enlargement as a treatment target. Their potential translational value is instead in phenotyping: when early TTE demonstrates RV enlargement, clinicians and investigators may consider a broader cardiopulmonary assessment rather than interpreting persistent lactate solely through LV systolic function or a single macrocirculatory variable. Prospective studies should combine serial lactate measurements with quantitative RV indices, venous-congestion markers, pulmonary vascular assessment, and treatment trajectories to determine whether this phenotype can improve physiological stratification or identify patients who benefit from specific hemodynamic strategies.

Key strengths are the explicit Lpre→E1→L24 temporal structure; adjustment for the lactate concentration immediately preceding echocardiography; a simple prespecified primary model; comparison with LVEF and other echocardiographic domains; and extensive sensitivity analyses addressing major clinical alternatives. Patient-level visualization and secondary model-form analyses provided additional information without redefining the primary estimand.

Several limitations should be considered. First, this was a single-center retrospective database study, so selection for early TTE and residual confounding may limit generalizability. Second, RV chamber size was derived from structured clinical reports rather than standardized quantitative measurements, and only 19 patients had severe enlargement. Third, complete information was unavailable for pulmonary vascular resistance, systemic venous congestion, RV strain, fractional area change, RV–pulmonary artery coupling, detailed treatment dose, and fine-grained continuous treatment timing. Fourth, selection of RV chamber size as the primary phenotype was informed by earlier exploratory work in the same database; although the time-ordered primary analysis was subsequently locked before rerunning, independent external validation is needed. Fifth, the secondary DML and quantile-regression analyses were intended as model-form and distributional checks, not separate confirmatory endpoints. Finally, an independent cohort with time-aligned lactate and structured RV measurements was not available for external validation.

In this time-ordered Sepsis-3 cohort, greater early RV chamber-size severity was associated with higher lactate burden several hours later after adjustment for pre-echocardiography lactate and clinical severity, whereas LVEF showed no comparable association. The findings support RV enlargement as a candidate cardiocirculatory phenotype linked to impaired subsequent metabolic recovery and motivate prospective, quantitative, and externally validated studies integrating cardiac phenotyping with lactate trajectories.

Declarations

Author contributions

YYZ and CJW conceived the study. YYZ developed the analytical approach, curated and analyzed the data, prepared the figures, and drafted the manuscript. JQW independently verified the analytic data and results and contributed to revision of the manuscript. XG and WB critically reviewed the manuscript, contributed to interpretation of the findings, and revised the manuscript for important intellectual

content. CJW supervised the study, provided project administration, contributed to interpretation of the findings, and critically revised the manuscript. All authors read and approved the final manuscript.

Funding

This work was supported by the Fundamental Research Funds for the Central Universities (Beijing University of Chinese Medicine; Grant No. 2025-JYB-JBGS-004) and by Tianjin Chase Sun Pharmaceutical Co., Ltd. through the commissioned project Multicenter Cohort Study of Xuebijing Injection for Sepsis Caused by Non-fermenting Bacteria, conducted under the Special Project for Technological Innovation in New Productive Forces of Modern Chinese Medicines (Grant No. 24ZXZKSY00050). The funders had no role in the design of the present MIMIC-based study, data analysis, interpretation of the results, manuscript preparation, or the decision to submit the work for publication.

Data availability

The data used in this study are available through PhysioNet as MIMIC-IV v3.1 and MIMIC-IV-Echo v1.0.1 to credentialed users who complete the required training and data-use procedures. Because these datasets are governed by PhysioNet access restrictions and data-use agreements, patient-level source data and derived patient-level records cannot be redistributed by the authors.

Code availability

Analytic code supporting the findings is available from the corresponding author upon reasonable request, subject to the applicable PhysioNet data-use requirements.

Competing interests

Caijun Wu reports institutional research funding from Tianjin Chase Sun Pharmaceutical Co., Ltd. through a commissioned research project related to Xuebijing Injection. The present study did not evaluate Xuebijing Injection, and the funder had no role in the design of this MIMIC-based study, data analysis, interpretation of the results, manuscript preparation, or the decision to submit the manuscript. The other authors declare no competing interests.

References

1. Evans, L. et al. Surviving sepsis campaign: international guidelines for management of sepsis and septic shock 2021. *Intensive Care Med.* **47** (11), 1181–1247. 10.1007/s00134-021-06506-y (2021).
2. Garcia-Alvarez, M., Marik, P. & Bellomo, R. Sepsis-associated hyperlactatemia. *Crit. Care*. **18** (5), 503. 10.1186/s13054-014-0503-3 (2014).
3. Hernández, G. et al. Effect of a resuscitation strategy targeting peripheral perfusion status vs serum lactate levels on 28-day mortality among patients with septic shock: the ANDROMEDA-SHOCK randomized clinical trial. *JAMA* **321** (7), 654–664. 10.1001/jama.2019.0071 (2019).

4. Castro, R., Hernández, G., Kattan, E. & Bakker, J. What every intensivist should know about the biphasic kinetics of lactate in septic shock. *J. Crit. Care*. **91**, 155286. 10.1016/j.jcrc.2025.155286 (2026).
5. Lakbar, I., Leone, M. & Muller, L. Decoding lactate kinetics in septic shock: From flow to metabolism. *J. Crit. Care*. **91**, 155287. 10.1016/j.jcrc.2025.155287 (2026).
6. Jones, A. E. et al. Lactate clearance vs central venous oxygen saturation as goals of early sepsis therapy: a randomized clinical trial. *JAMA* **303** (8), 739–746. 10.1001/jama.2010.158 (2010).
7. Beesley, S. J. et al. Septic Cardiomyopathy. *Crit. Care Med.* **46** (4), 625–634. 10.1097/CCM.0000000000002851 (2018).
8. Wang, J., Tong, Z., Wang, X. & Wang, G. Time Course of Morbidity and Mortality Across Echocardiographic Phenotypes in Patients With Sepsis: A Systematic Review and Meta-Analysis. *Crit. Care Med.* **53** (11), e2294–e2304. 10.1097/CCM.0000000000006844 (2025).
9. Mukherjee, M. et al. Guidelines for the Echocardiographic Assessment of the Right Heart in Adults and Special Considerations in Pulmonary Hypertension. *J. Am. Soc. Echocardiogr*. **38** (3), 141–186. 10.1016/j.echo.2025.01.006 (2025).
10. Lanspa, M. J. et al. Right Ventricular Dysfunction in Early Sepsis and Septic Shock. *Chest* **159** (3), 1055–1063. 10.1016/j.chest.2020.09.274 (2021).
11. Vallabhajosyula, S. et al. Impact of Right Ventricular Dysfunction on Short-term and Long-term Mortality in Sepsis: A Meta-analysis of 1,373 Patients. *Chest* **159** (6), 2254–2263. 10.1016/j.chest.2020.12.016 (2021).
12. Shvilkina, T. et al. Echocardiographic phenotypes in sepsis: identifying subgroups using latent profile analysis. *J. Intensive Care*. **14**, 37. 10.1186/s40560-026-00873-8 (2026).
13. Jin, L. et al. Lactate-right ventricular discordance patterns and mortality in critical illness. *BMC Cardiovasc. Disord*. 10.1186/s12872-026-06440-1 (2026).
14. Johnson, A. E. W. et al. MIMIC-IV, a freely accessible electronic health record dataset. *Sci. Data*. **10**, 1. 10.1038/s41597-022-01899-x (2023).
15. Gow, B. et al. MIMIC-IV-Echo: Echocardiogram Matched Subset (version 1.0.1). PhysioNet. (2026). 10.13026/307c-mr50
16. Singer, M. et al. The Third International Consensus Definitions for Sepsis and Septic Shock (Sepsis-3). *JAMA* **315** (8), 801–810. 10.1001/jama.2016.0287 (2016).
17. Lang, R. M. et al. Recommendations for cardiac chamber quantification by echocardiography in adults. *J. Am. Soc. Echocardiogr*. **28** (1), 1–39e14. 10.1016/j.echo.2014.10.003 (2015).
18. Koenker, R. & Bassett, G. Jr. Regression quantiles. *Econometrica* **46** (1), 33–50. 10.2307/1913643 (1978).
19. Chernozhukov, V. et al. Double/debiased machine learning for treatment and structural parameters. *Econom J.* **21** (1), C1–C68. 10.1111/ectj.12097 (2018).

20. Aalen, O. O. & Johansen, S. An empirical transition matrix for non-homogeneous Markov chains based on censored observations. *Scand. J. Stat.* **5**, 141–150 (1978).
21. von Elm, E. et al. The STROBE statement: guidelines for reporting observational studies. *Lancet* **370** (9596), 1453–1457. 10.1016/S0140-6736(07)61602-X (2007).
22. Benchimol, E. I. et al. The RECORD statement. *PLoS Med.* **12** (10), e1001885. 10.1371/journal.pmed.1001885 (2015).
23. Vieillard-Baron, A. et al. Right ventricular failure in septic shock: characterization, incidence and impact on fluid responsiveness. *Crit. Care*. **24**, 630. 10.1186/s13054-020-03345-z (2020).
24. Boissier, F. & Aissaoui, N. Septic cardiomyopathy: Diagnosis and management. *J. Intensive Med.* **2** (1), 8–16. 10.1016/j.jointm.2021.11.004 (2022).
25. Cavefors, O., Bech-Hanssen, O., Redfors, B. & Oras, J. Echocardiographic assessment of left ventricular longitudinal function in critically ill patients. *Crit. Care*. **30**, 365. 10.1186/s13054-026-06193-5 (2026).
26. Vallabhajosyula, S. et al. Prognostic impact of isolated right ventricular dysfunction in sepsis and septic shock: an 8-year historical cohort study. *Ann. Intensive Care*. **7**, 94. 10.1186/s13613-017-0319-9 (2017).
27. Sanfilippo, F. et al. Diastolic dysfunction and mortality in septic patients: a systematic review and meta-analysis. *Intensive Care Med.* **41** (6), 1004–1013. 10.1007/s00134-015-3748-7 (2015).
28. Wei, Y. et al. Lactate trajectories and outcomes in patients with sepsis in the intensive care unit: group-based trajectory modeling. *Front. Public. Health*. **13**, 1610220. 10.3389/fpubh.2025.1610220 (2025).
29. Li, X. et al. Joint lactate and vasoactive-inotropic score trajectories and post-landmark mortality in sepsis: a retrospective cohort study in MIMIC-IV. *BMC Cardiovasc. Disord*. 10.1186/s12872-026-06588-w (2026).

Figures

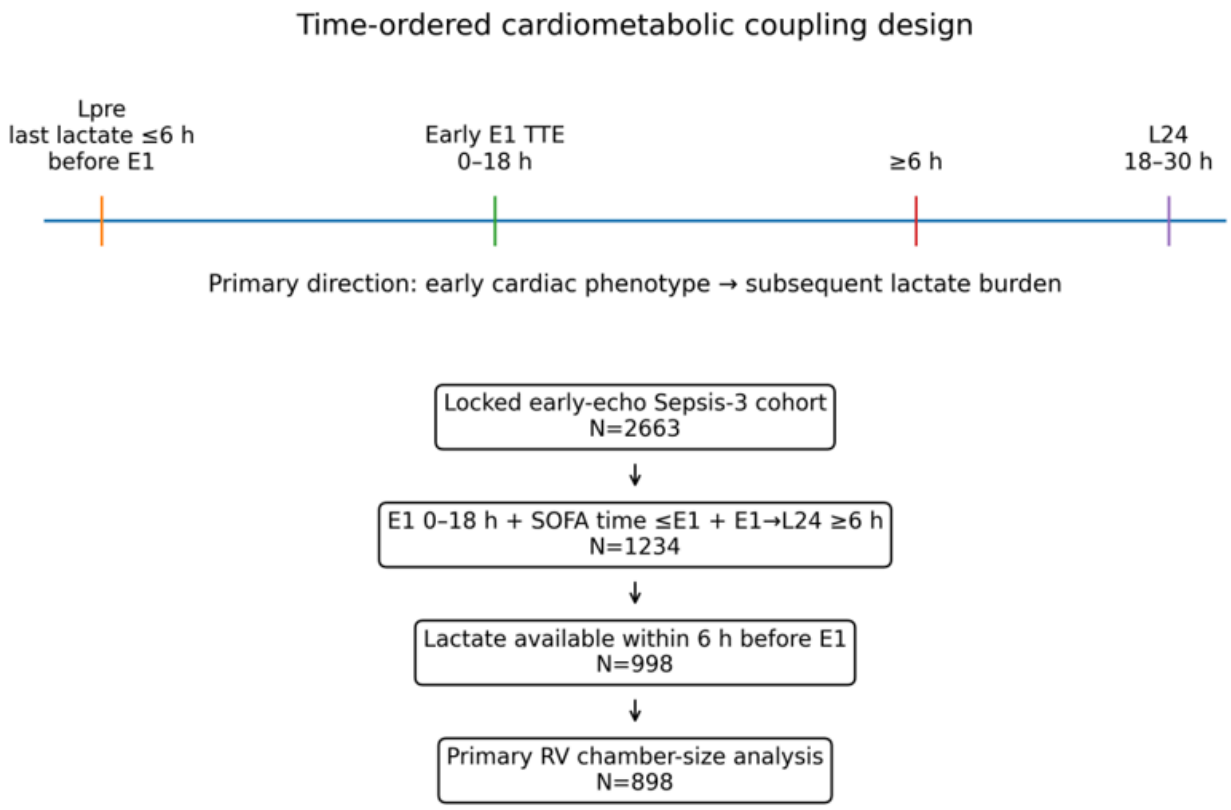

Figure 1

Time-ordered study design and analytic cohorts.

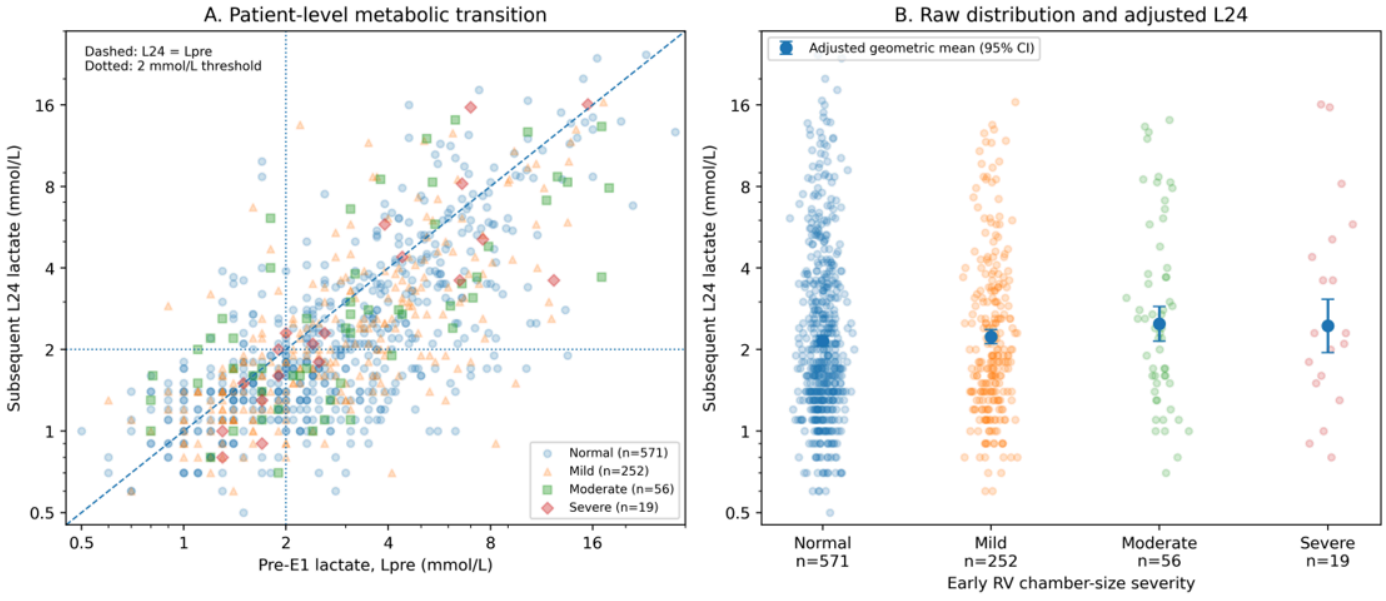

Figure 2

Patient-level lactate transition according to early RV chamber-size grade. (A) Patient-level scatterplot of the most recent pre-E1 lactate (Lpre) versus subsequent L24; the dashed diagonal denotes L24=Lpre and the dotted lines denote the 2-mmol/L threshold. (B) Raw L24 distribution and covariate-adjusted marginal geometric means (95% CI) across RV structural grades. The y-axis is shown on a logarithmic scale to display the high-lactate tail.

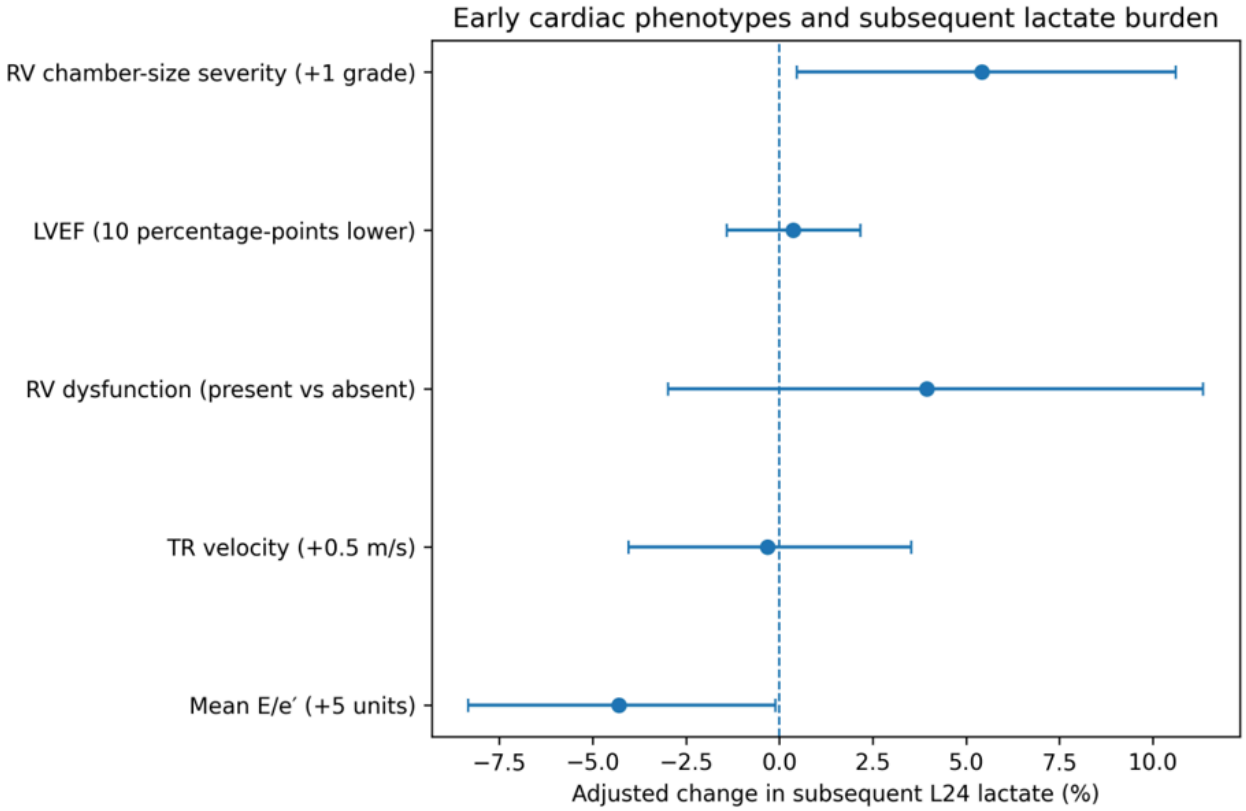

Figure 3

Adjusted associations of early cardiac phenotypes with subsequent L24 lactate burden.

Secondary model-form and distributional analyses

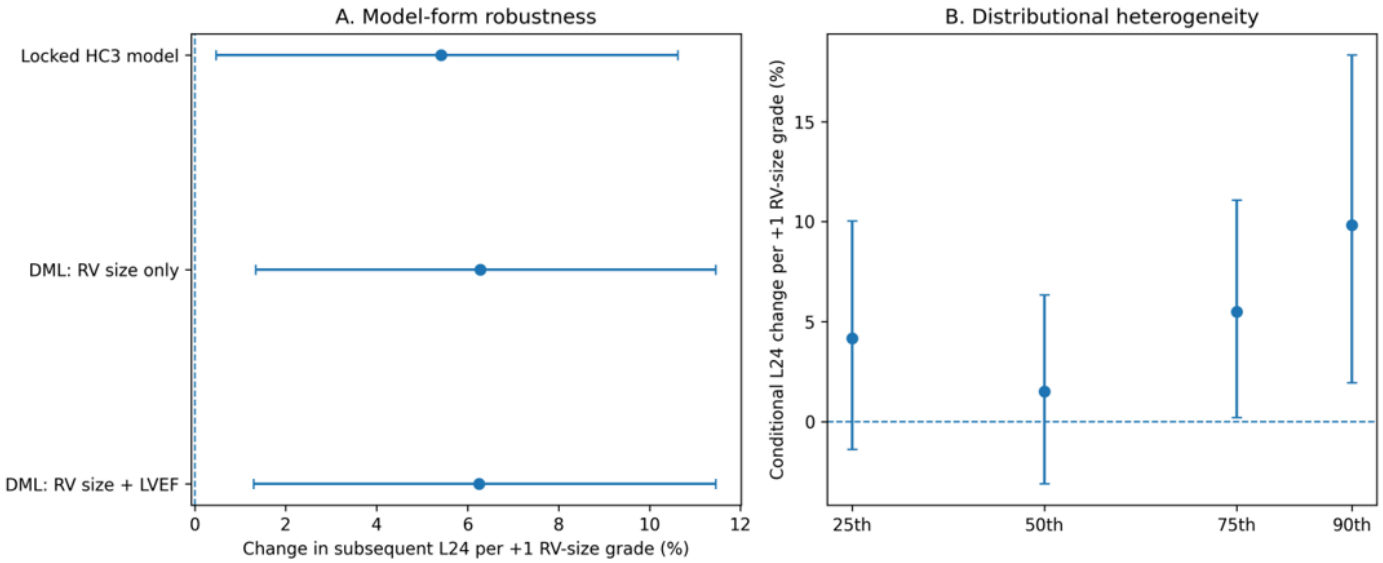

Figure 4

Model-form robustness of the conventional primary model and double machine learning, and associations of RV chamber size with different conditional quantiles of subsequent L24.

Supplementary Files

This is a list of supplementary files associated with this preprint. Click to download.

- Supplementary.docx